Supporting Information: "Highly tunable elastic dielectric metasurface lenses"

Seyedeh Mahsa Kamali, Ehsan Arbabi, Amir Arbabi, Yu Horie, and Andrei Faraon

SUPPLEMENTARY NOTE 1: SAMPLING FREQUENCY OF THE PHASE PROFILE

The lattice constant should be chosen such that the lattice remains non-diffractive and satisfies the Nyquist sampling criterion. From a signal processing point of view, the locally varying transmission coefficient of a flat microlens can be considered as a spatially band-limited signal with a $2\mathrm{NA}k_0$ bandwidth (ignoring the effect of the edges), where NA is the microlens numerical aperture, and k_0 is the vacuum wavenumber. A hypothetical one dimensional band-limited spectrum is depicted in Fig. S1 (solid blue curve). By sampling the microlens phase profile with sampling frequency of K_s, the images (dashed blue curves in Fig. S1) are added to the spectrum. Therefore, for the perfect reconstruction of the microlens' transmission coefficient, the Nyquist criterion should be satisfied: $K_s > 2\mathrm{NA}k_0$. On the other hand, the lattice should remain subwavelength; the higher order diffractions (dashed blue curves in Fig. S1) should remain non-propagating. Propagation in free space can be considered as a low pass filter with $2nk_0$ bandwidth (solid red curve in Fig. S1), where n is the refractive index of the surrounding medium. Therefore, in order to have perfect reconstruction of phase and non-propagating higher order diffractions, the following relation should be satisfied:

$$K_s > nk_0 + \mathrm{NA}k_0 \tag{1}$$

Note that the sampling frequency (K_s) is a reciprocal lattice vector. For the square lattice $K_s = 2\pi/\Lambda$, where Λ is the lattice constant. Therefore Eq. (1) would be simplified as follows:

$$\Lambda < \frac{\lambda}{n + \mathrm{NA}} \tag{2}$$

Where λ is the free space wavelength. Note that the maximum value of numerical aperture is $\mathrm{NA}_{\max} = n$, which simplifies Eq. (2) to $\Lambda < \lambda/(2n)$. For designing tunable microlenses, Eq. (2) should be satisfied for all the strains of interest, and $\Lambda = (1 + \epsilon)a$, where a is the unstrained lattice constant. For the parameters used in the main text, the unstrained lattice constant should be smaller than 401 nm in order to have tunable microlens up to 50% strains. The unstrained lattice constant was chosen to be 380 nm.

SUPPLEMENTARY FIGURES

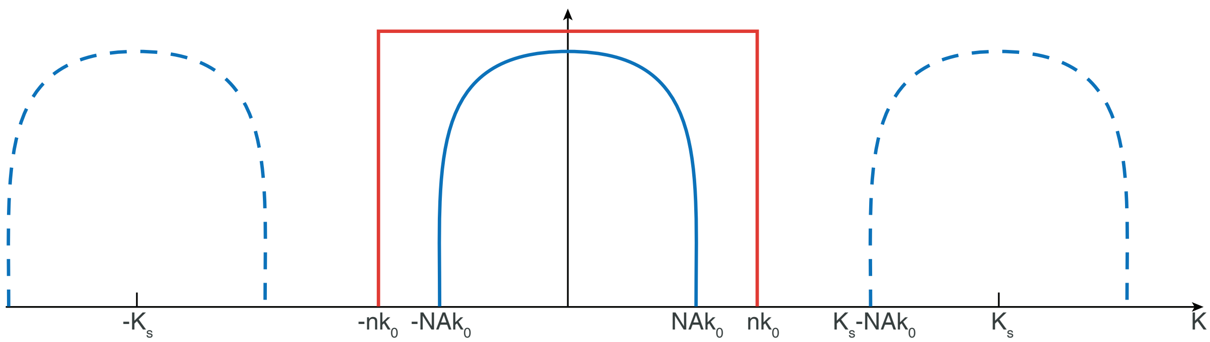

Figure S1. Sampling frequency of the phase profile for perfect reconstruction of the wavefront. The locally varying transmission coefficient spectrum of a flat microlens can be considered as a band-limited signal with $2\mathrm{NA}k_0$ bandwidth (solid blue curve). By sampling the transmission coefficient with sampling frequency of K_s, displaced copies of the band-limited signal are added to the spectrum (dashed blue curves). In order to avoid undesirable diffractions, the free space low pass filter (solid red curve) should only filter the zeroth order diffraction (solid blue curve).

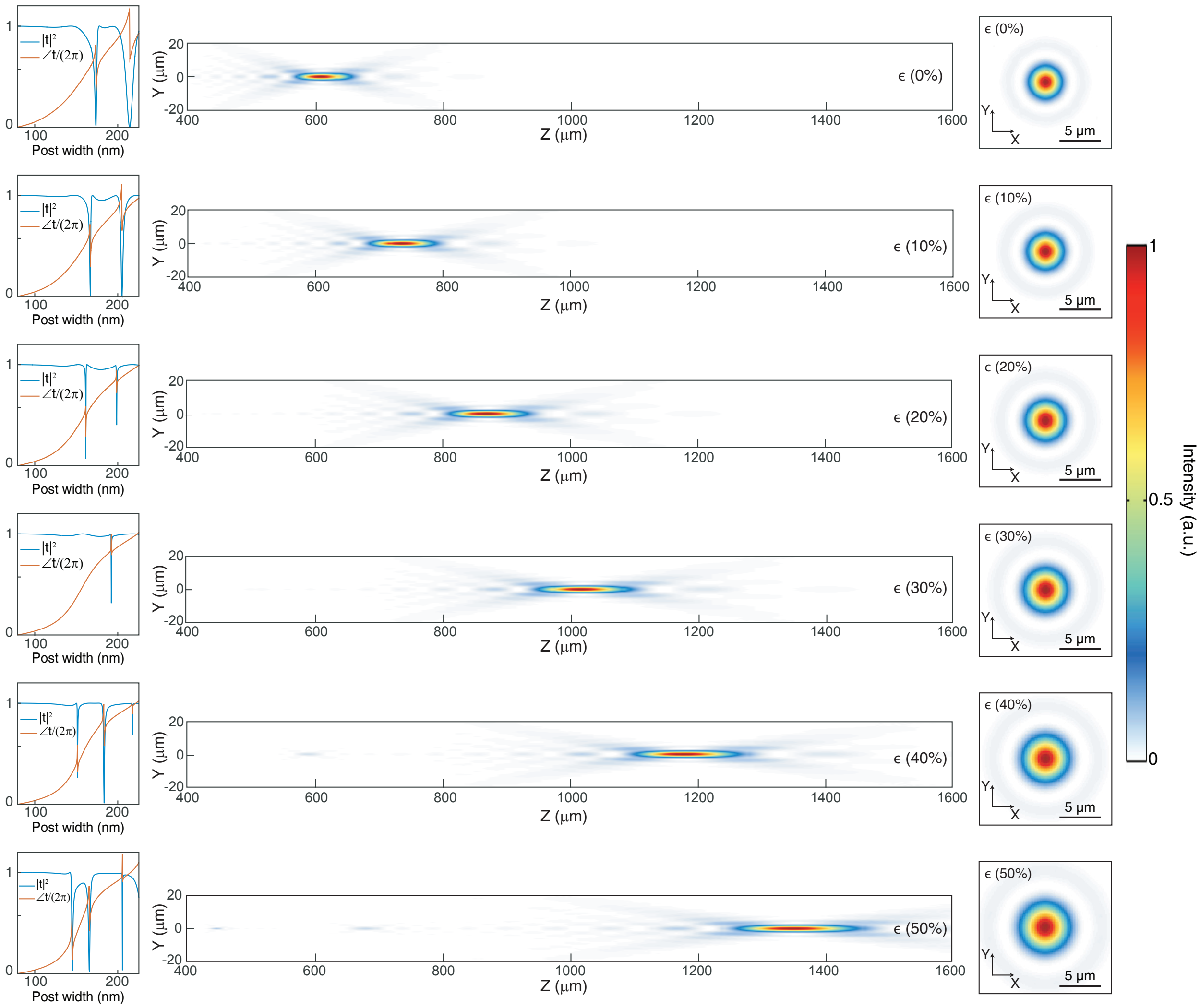

Figure S2. Simulation results of the tunable microlens using the actual nano-posts' transmission coefficients, extracted from Figs. 2b and 2c in the main text. Intensity profiles of the tunable microlens are simulated at different strains ($\epsilon = 0\%$ to 50%) using the actual transmission coefficients at each strain value. Intensity and phase of the transmission coefficient at respective strain values are shown in the left, and their corresponding intensity profiles in the axial plane and in the focal plane are shown in the middle and right, respectively.

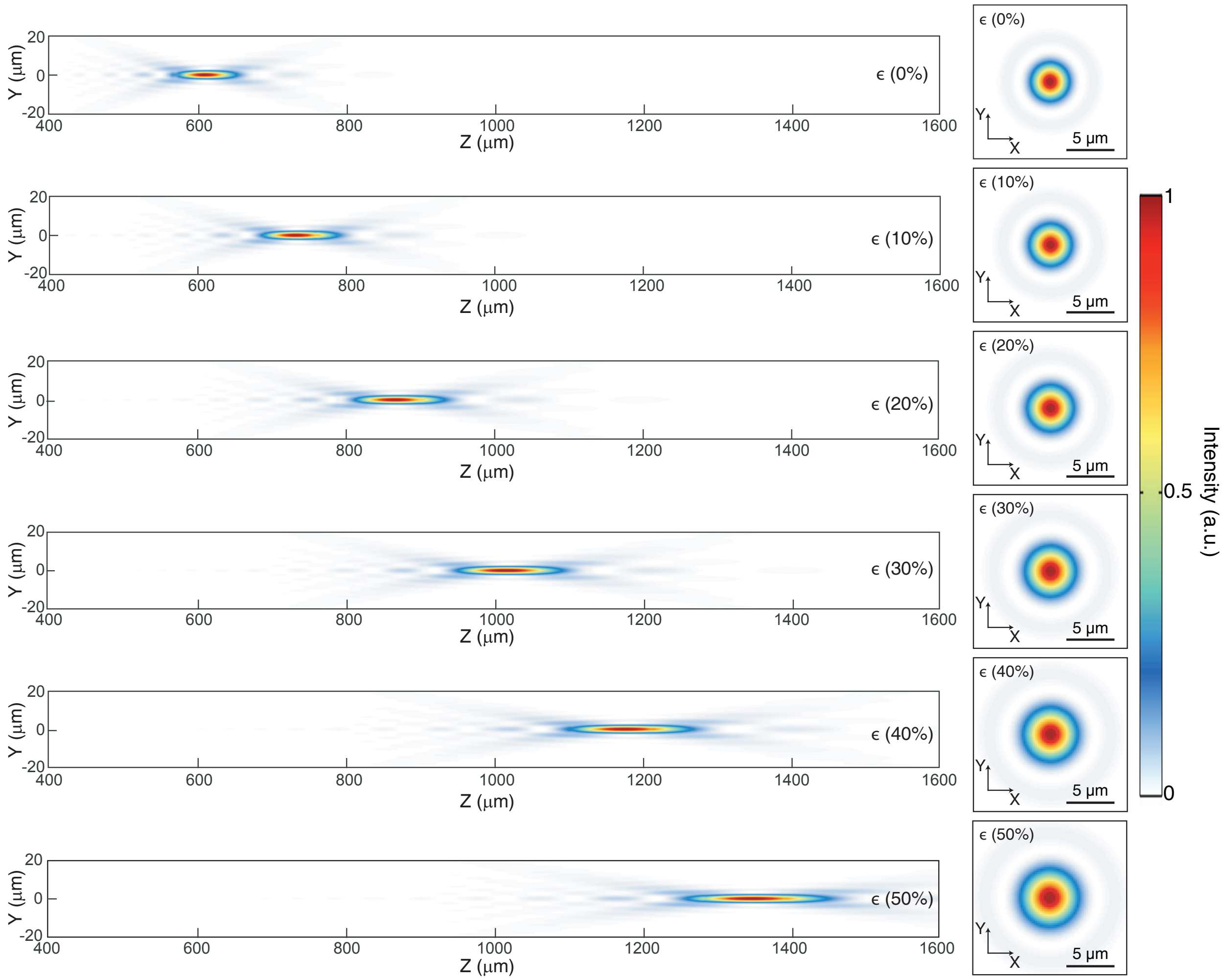

Figure S3. Simulation results of the tunable microlens assuming transmission coefficients that do not change with strain. We have used the simulated nano-post transmission coefficients at the strain value of 25% (main text, Fig. 2d) for all strains. Simulated intensity profiles for different strains (ϵ = 0% to 50%) are shown in the axial plane (left) and in the focal plane (right).

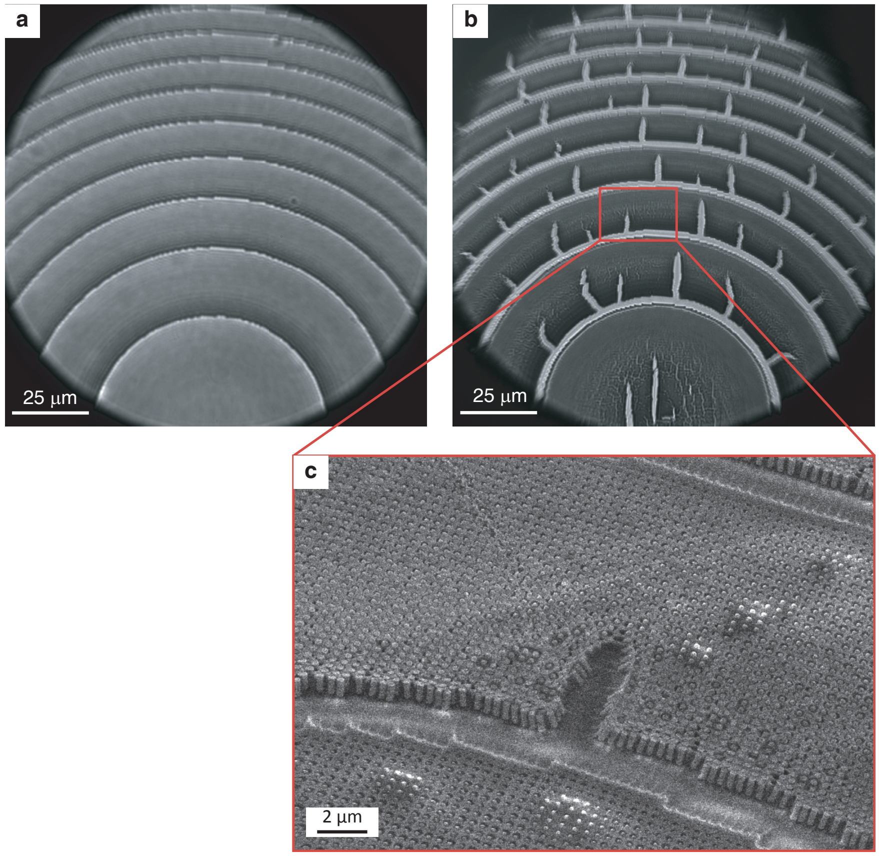

Figure S4. Importance of PDMS cladding in the performance of the elastic metasurface under high strains. Optical images of the nano-posts in PDMS with (a) and without the PDMS claddings (b) under $\sim$50% radial strain. The images are taken using the same measurement setup shown in Fig. 4(a) under green laser illumination. Elastic metasurface without the PDMS cladding stretches non-uniformly, and some cracks are formed at the borders of the small and large nano-posts starting at $\sim$25% strain. By increasing the strain, these cracks spread in the elastic metasurface and some of the nano-posts stick out of the PDMS. (c) Scanning electron micrograph of the nano-posts without the PDMS cladding under $\sim$50% radial strain, taken at a tilt angle of 30 degrees. a $\sim$10-nm-thick gold layer was deposited on the sample to dissipate charge accumulation during the scanning electron imaging. The metasurface microlens presented in the main manuscript has PDMS cladding, and its nano-posts are completely encapsulated inside a thin PDMS layer. In this manner, the cracks do not show up between the nano-posts even at very high strains (as shown in (a)).

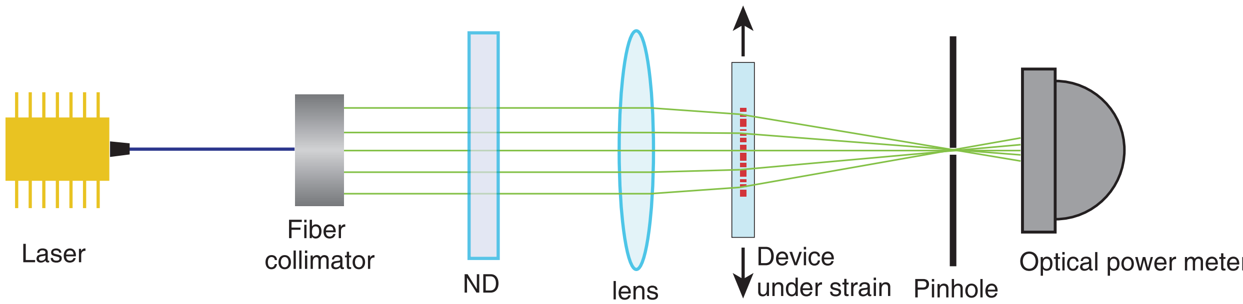

Figure S5. Schematic illustration of the measurement setup used for measuring the efficiencies of the tunable microlens. ND: neutral density filter.

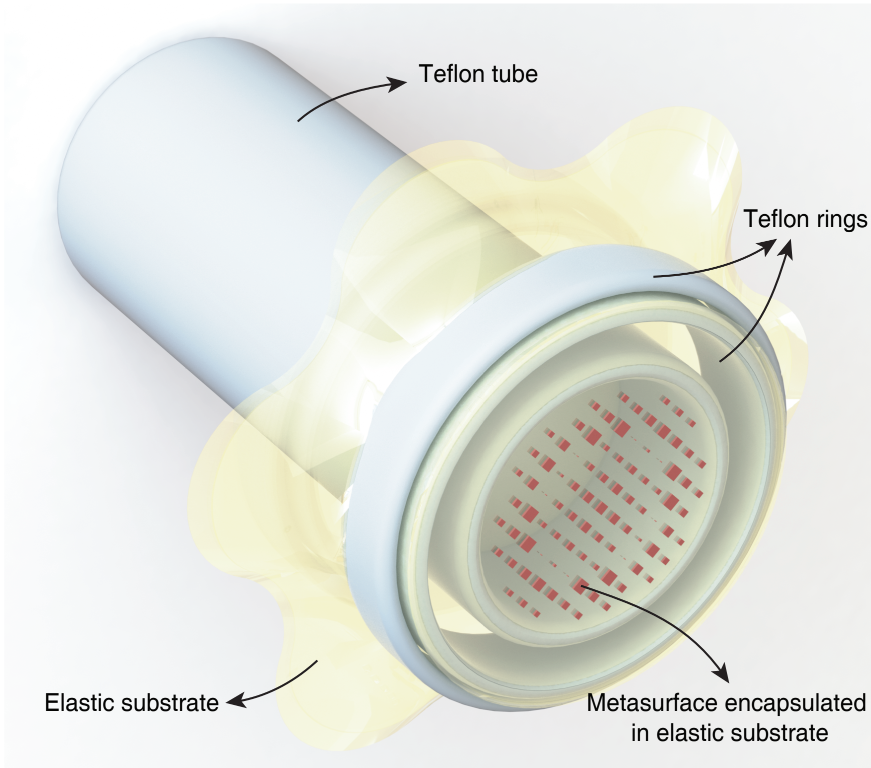

Figure S6. Schematic illustration of the method used for radially stretching the elastic metasurface. The elastic metasurface is fixed between the Teflon rings and is stretched radially by pushing the Teflon tube against it from the backside.

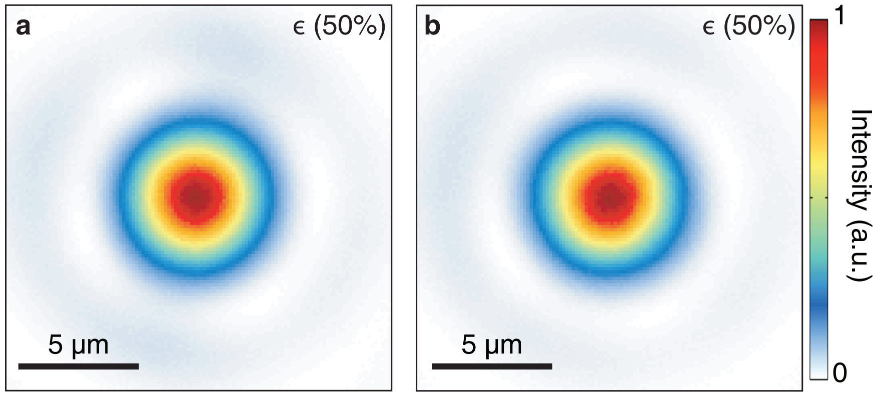

Figure S7. Reliability measurement of the microlens under strain. Measured optical intensity profile of the tunable microlens in the plane of focus under 50% strain after one (a), and more than ten times of stretching and releasing the device (b).

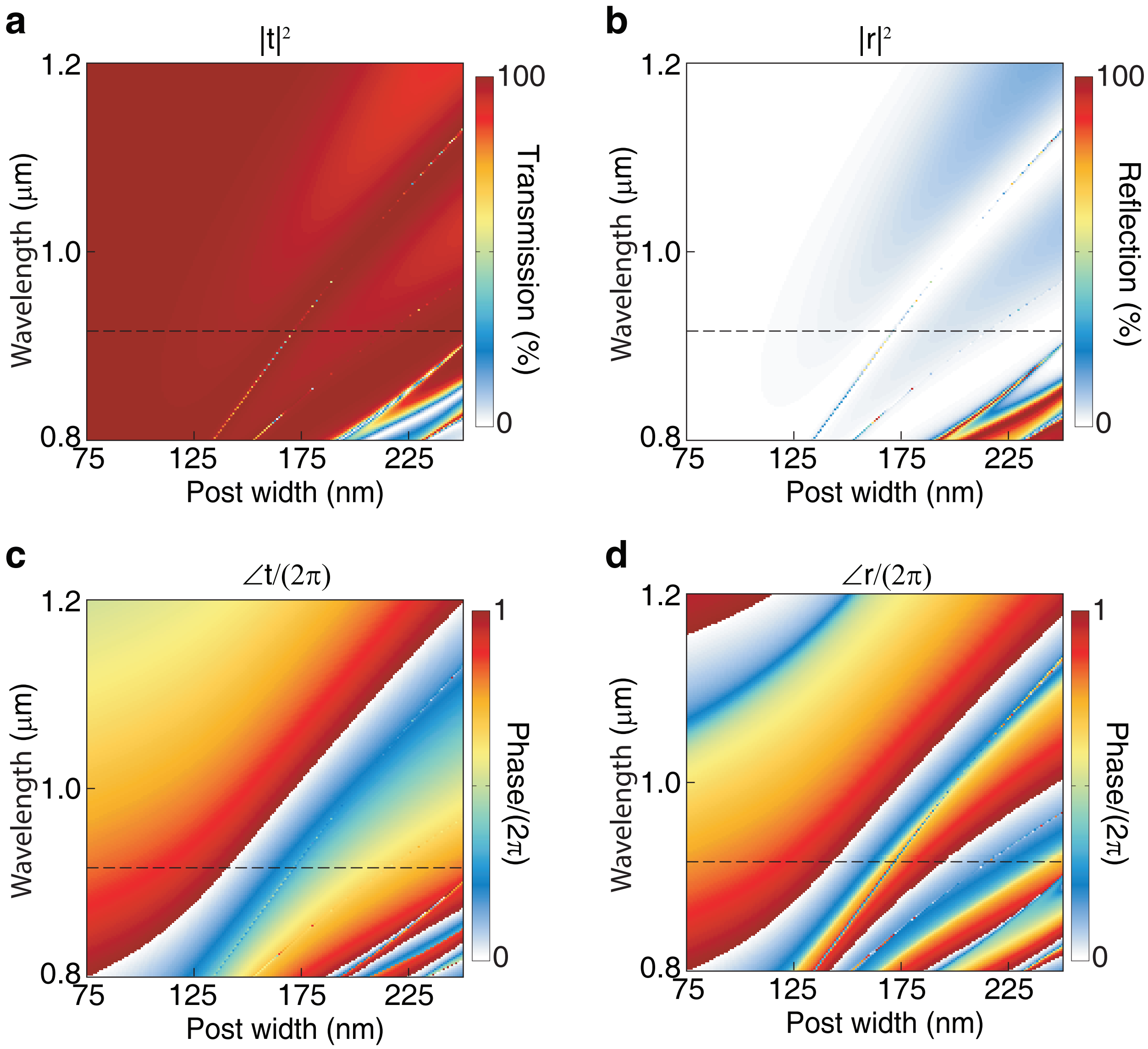

Figure S8. Simulated transmittance and reflection spectra of uniform array of nano-posts. (a) Simulated intensity and (c) phase of the transmission coefficient for the array shown in Fig. 2(a) as a function of the nano-post width at 25% strain. (b) Reflection intensity and (d) phase of the reflection coefficient for the same structure. Black dashed lines indicate the simulation wavelength of 915 nm, which is used in this manuscript.